JOURNAL OF CHEMICAL INFORMATION AND MODELING

Article

pubs.acs.org/jcim

Cyclophilin A Inhibition: Targeting Transition-State-Bound Enzyme Conformations for Structure-Based Drug Design

Mulpuri Nagaraju, Lauren C. McGowan, and Donald Hamelberg*

Department of Chemistry and Center for Biotechnology and Drug Design, Georgia State University, Atlanta, Georgia 30302-4098, United States

Supporting Information

ABSTRACT: Human Cyclophilin A (CypA) catalyzes cis−trans isomerization of the prolyl peptide ω-bond in proteins and is involved in many subcellular processes. CypA has, therefore, been identified as a potential drug target in many diseases, and the development of potent inhibitors with high selectivity is a key objective. In computer-aided drug design, selectivity is improved by taking into account the inherent flexibility of the receptor. However, the relevant receptor conformations to focus on in order to develop highly selective inhibitors are not always obvious from available X-ray crystal structures or ensemble of conformations generated using molecular dynamics simulations. Here, we show that the conformation of the active site of CypA varies as the substrate configuration changes during catalytic turnover. We have analyzed the principal modes of the active site dynamics of CypA from molecular dynamics simulations to show that similar ensembles of enzyme conformations recognize diverse inhibitors and bind the different configurations of the peptide substrate. Small nonpeptidomimetic inhibitors with varying activity are recognized by enzyme ensembles that are similar to those that tightly bind the transition state and cis configurations of the substrate. Our results suggest that enzyme−substrate ensembles are more relevant in structure-based drug design for CypA than free enzyme. Of the vast conformational space of the free enzyme, the enzyme conformations of the tightly bound enzyme−substrate complexes are the most important for catalysis. Therefore, functionalizing lead compounds to optimize their interactions with the enzyme's conformational ensemble bound to the substrate in the cis or the transition state could lead to more potent inhibitors.

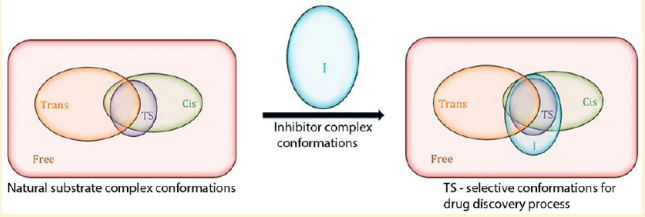

INTRODUCTION

Cyclophilin A (CypA) is a member of the immunophilin family of enzymes[1] that play critical roles in various biological processes, such as enhancing the rate of protein folding (or unfolding) via its peptidyl-prolyl isomerase (PPIase) activity.[2,3] CypA is an important drug target for cyclosporine A (CsA), an immunosuppressive inhibitory drug that is widely used to prevent organ rejection after transplant operation.[4] CypA performs an essential function during the maturation of the HIV-1 virus, catalyzing cis−trans isomerization of a -Gly-Pro- motif on an exposed loop of the HIV-1 capsid monomer in order to facilitate viral replication.[5,6] Recent studies show that CypA is overexpressed in many cancer cells, such as human pancreatic cancer cells, oral squamous cancer cells, endometrial carcinoma, and nonsmall cell lung cancer cells.[7−10] CypA also binds to the nucleocapsid protein of SARS coronavirus, which causes infection, and CypA induces neuroprotective or neurotrophic effects when present at high levels in the brain.[11−13] Due to the involvement of CypA in the regulation of numerous biological processes and related diseases, CypA has been identified as a potential drug target. Therefore, significant efforts have been put into discovering potent CypA inhibitors and discriminating between different isoforms of Cyclophilin.[14−16] Well-known inhibitors of CypA, such as CsA and sanglifehrin A, were derived mainly from natural products and peptide analogues[1,17−19] and tend to have low solubility in water and serious side effects.[20]

Along with in vitro drug synthesis, computational docking and virtual screening methods have become an integral part of structure-based drug design and play important roles in developing new drug candidates.[21] In traditional docking and virtual screening methods, a single or few X-ray crystal structures (or homologous structures) are used along with a fully flexible ligand.[22−25] In recent years, the flexibility of the receptor's active site is taken into consideration by allowing for small movements in the protein backbone and significant changes in the rotameric states of the amino acid side chains.[26−29] Furthermore, large-scale conformational rearrangements of the receptor can be achieved a priori using one of many conformational sampling techniques, such as molecular dynamics (MD) simulation.[30] These approaches, which are normally referred to as ensemble docking or relaxed complex methods,[31−33] use a diverse ensemble of conformations of the receptor and provide a probability distribution of binding free energies or scores for a particular ligand. The diversity of the receptor conformations will depend on the extent of sampling and whether the relevant conformations are readily accessible

Received: September 12, 2012
Published: January 13, 2013

   dx.doi.org/10.1021/ci300432w | J. Chem. Inf. Model. 2013, 53, 403−410

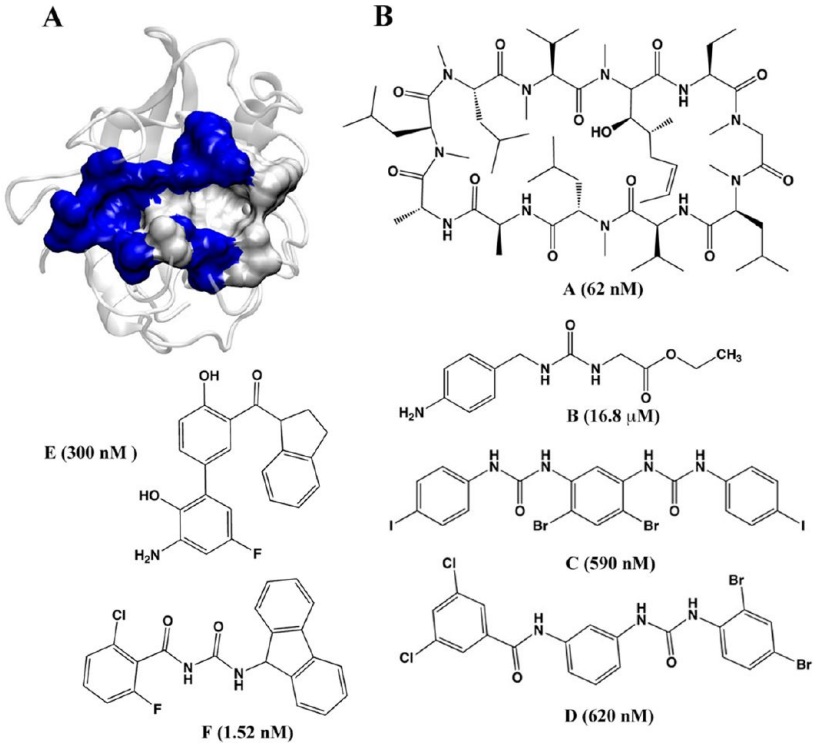

Figure 1. Active site of Cyclophilin A and known inhibitors: (A) active site of CypA consisting of a polar pocket (blue surface) and a nonpolar pocket (white surface), connected by a channel that is partially polar. (B) Chemical structures of inhibitors considered in this study (A,[41] B,[44] C, D,[43] E,[14] F[42]) with their IC_{50} values in parentheses. The K_i, instead of the IC_{50}, is reported for compound E.

by the free receptor. Nonetheless, relaxed complex approaches have been shown to do better in identifying potent inhibitors than approaches that use a single or few conformations of X-ray crystal structures.[34−38] Additionally, it has been suggested that the performance or predictive power of virtual screening can be improved by using an ensemble of receptor conformations that were generated in complex with bound ligands or substrates.[39] One could therefore argue that the ligand or substrate induces a subset of pertinent conformations in the binding site that are poorly or never sampled in the free receptor. Therefore, obtaining and identifying the relevant ensemble of enzyme conformations for rational drug design is critical to the development of potent inhibitors. However, because of the hyper-dimensional landscape of biomolecules, the conformational sampling of the free receptor is not always exhaustive.

In an enzyme, the ensemble of accessible conformations could depend on the conformational states of the natural substrate. In CypA, for example, the substrate can exist in the cis, trans, or transition state configurations during catalytic turnover, and the X-ray crystal structures may not be representative of the different ensembles of enzyme conformations that bind the substrate in the different configurations. Also, unless the conformational sampling of the substrate-free receptor, using MD or some other methods, is exhaustive, there is the possibility that relevant ensembles of conformations in the catalytic pathway that may prove useful for inhibitor design may not be adequately sampled. Therefore, there is a need to reliably and efficiently access these conformations, especially if the active site of the enzyme significantly rearranges during catalytic turnover. Is it necessary to consider all of the possible conformations of the free enzyme or is there a subset of conformations that is the most relevant for designing potent inhibitors? For example, transition state analogues (mimics) have always been designed and used as potent inhibitors.[40] The extent to which an enzyme stabilizes the transition state relative to reactants and products determines the efficiency of the enzyme. Therefore, a small molecule that can bind to the enzyme's transition state ensemble of conformations can reduce the overall activity of the enzyme. Is the ensemble of enzyme conformations that recognizes the transition state the most relevant in designing potent inhibitors?

To answer these questions, we have used human CypA as a case study and carried out all-atom molecular dynamics simulations on the substrate-free enzyme, the enzyme−substrate (Ace-Ala-Ala-Pro-Phe-Nme) complexes when the peptide ω-bond angle of the -Ala-Pro- motif is in the cis (0°), transition state (90°), and trans (±180°) configurations, and six enzyme−inhibitor complexes. The transition state and the other configurations of the substrate of CypA are reliably defined, since there is no bond formation or breakage during the catalytic process. Six previously reported small active nonpeptidomimetic inhibitors[14,41−44] (Figure 1) are used in this study. The activities (IC_{50}) of these inhibitors are in the nanomolar to micromolar range.

RESULTS AND DISCUSSION

We have analyzed the trajectories of ten molecular dynamics simulations in order to probe the motions of ensembles of conformations of the active site of CypA in its substrate-free, substrate-bound, and inhibitor-bound states. The substrate-free simulation of CypA was carried out for 340 ns, and three substrate-bound simulations of CypA were carried out, each for 50 ns, with the peptide ω-bond angle of the -Ala-Pro- motif of the Ace-Ala-Ala-Pro-Phe-Nme substrate analogue in the trans, transition state, and cis configurations. Six inhibitor-bound

dx.doi.org/10.1021/ci300432w | J. Chem. Inf. Model. 2013, 53, 403−410

CypA complexes were also simulated for 30 ns each, using the six inhibitors listed in Figure 1.

Conformational Changes in the Active Site of Cyclophilin A. The active site of CypA comprises a hydrophobic proline binding pocket and a polar pocket that are connected by a narrow partially polar channel, as shown in Figure 1. We have characterized the dynamical motions of the active site residues of CypA in the absence and presence of the peptide substrate analogue. The trajectories of the bound and unbound simulations were analyzed using principal component analysis (PCA) to determine the top principal modes (eigenvectors) that represent the dominant motions of the active site. Projections of the top three slowest modes that represent the majority of the total fluctuation of the active site residues are shown in Figure 2. The conformations of the active site

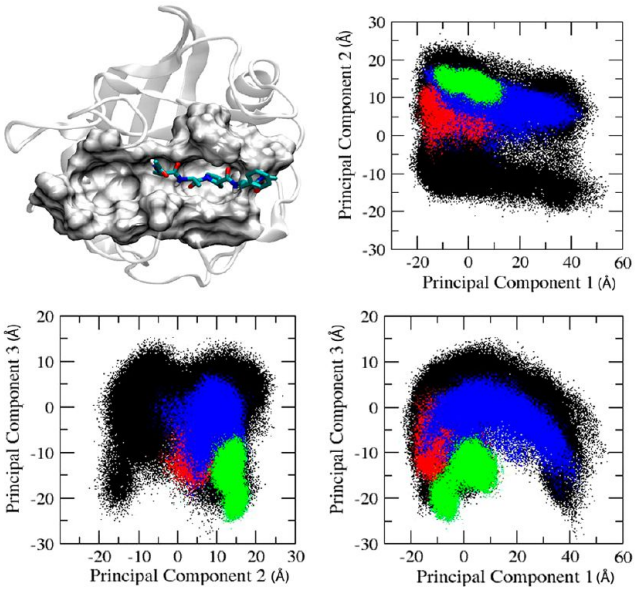

Figure 2. Top three principal component of the active site residues of the different CypA ensembles: (free) black, (cis) red, (transition state) green, and (trans) blue. The active site residues are Arg 55, Phe 60, Met 61, Gln 63, Gly 74, Gly 75, Glu 81, Lys 82, Ala 101, Asn 102, Ala 103, Thr 107, Gly 109, Ser 110, Gln 111, Phe 113, Leu 122, and His 126. The substrate analogue (Ace-Ala-Ala-Pro-Phe-Nme) is in the transition state configuration.

residues of the substrate-free enzyme contain the conformations that can bind the trans, cis, and transition state configurations of the substrate. The conformations of the bound enzyme are intrinsic to and are present in the free enzyme. Each data point shown in Figure 2 represents a conformation of the active site in the free, trans, transition state, and cis ensembles.

The enzyme conformations that bind the substrate in the trans, cis, and transition state configurations of the substrate are distinguishable (Figure 2), with some overlapping regions. These results suggest that the active site of the free enzyme can easily change its shape to accommodate the different states of the substrate during catalytic turnover, favoring mainly conformational selection.[45] It appears that the binding site of the enzyme has evolved to be inherently plastic with a notable decrease in the fluctuation of the transition state ensemble. The considerable loss in plasticity is attributed to well-formed intermolecular interactions, both polar and nonpolar between the enzyme and the substrate at the transition state. We previously estimated the binding free energies of each ensemble corresponding to the complex of enzyme with the substrate in different configurations using the MM/PBSA (molecular mechanics Poisson−Boltzmann surface area) approach.[46] We found that the transition state of the substrate binds better than the cis, and the cis binds better than trans configuration.[47] These results indicate that the enzyme is preorganized to bind the transition state configuration of the substrate better than the cis and trans configurations, as was previously shown.[48]

Potent Inhibitors Are Recognized by Functionally Relevant Active Site Conformations of CypA. CypA−inhibitor complexes of six previously reported inhibitors (A−F in Figure 1) were used to study the conformational preference of the active site upon ligand binding. The binding modes of the inhibitors in the active site of CypA are shown in Figure 3.

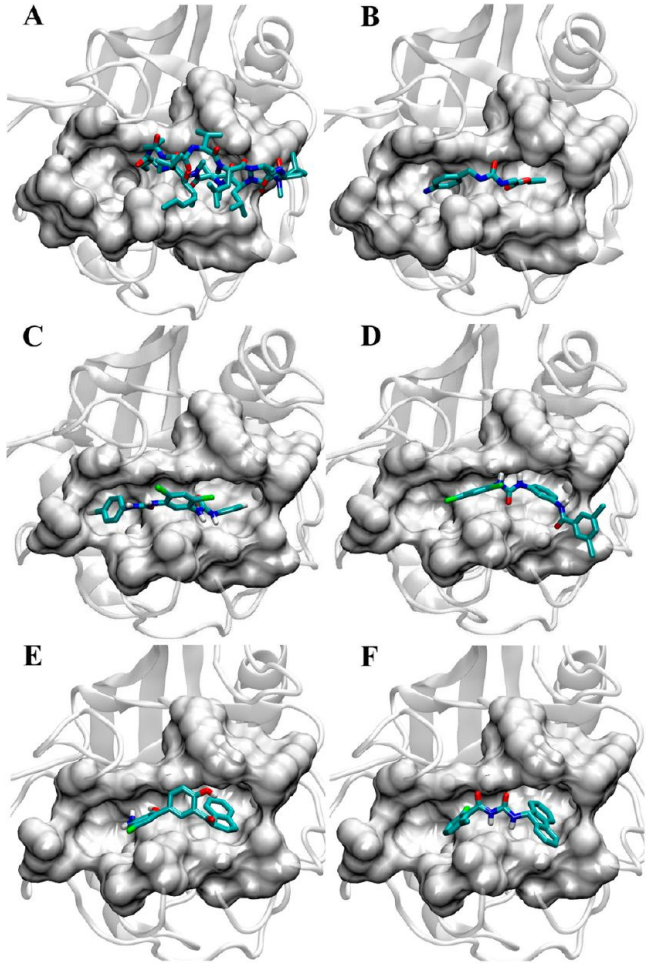

Figure 3. Binding modes of the different inhibitors of CypA. The binding modes of compounds A and B are taken from the crystal structures with PDB ID 1CWA and 3RDD, respectively. The most probably binding modes for the compounds C−F were obtained using AutoDock Vina.

Crystal structures are available for inhibitors A and B. The binding modes of C−F were obtained by docking the inhibitors into the active site of an ensemble of conformations of CypA using AutoDock Vina[49] and identifying the binding mode with the most probable binding affinity. Compounds A and B were redocked into the active site of the respective crystal structures and an ensemble of conformations of CypA that was generated

dx.doi.org/10.1021/ci300432w | J. Chem. Inf. Model. 2013, 53, 403−410

using molecular dynamics. The resulting binding modes were similar to those in the crystal structures (Supporting Information Figure S1). The binding site of CypA consists of the proline binding nonpolar cavity and an adjacent polar cavity, separated by a partially polar channel, as shown in Figure 1. In all cases, nonpolar groups (phenyl or fused-rings) occupy the nonpolar pocket, whereas polar groups occupy the channel and the polar pocket. These structures were used as starting structures for 30 ns of molecular dynamics simulations for each compound. The last 20 ns were used for analysis. The initial positions of the compounds were not significantly altered during the simulations, except for compound C.

Principal components analysis was carried out on all atoms of active site residues of CypA to identify the overall patterns of motions upon binding the inhibitors. Projection of the top three eigenvectors accounts for more than 75% of all motions in the free enzyme. The top three principal components of compounds A–F are shown in Figure 4. Figure 4 shows that

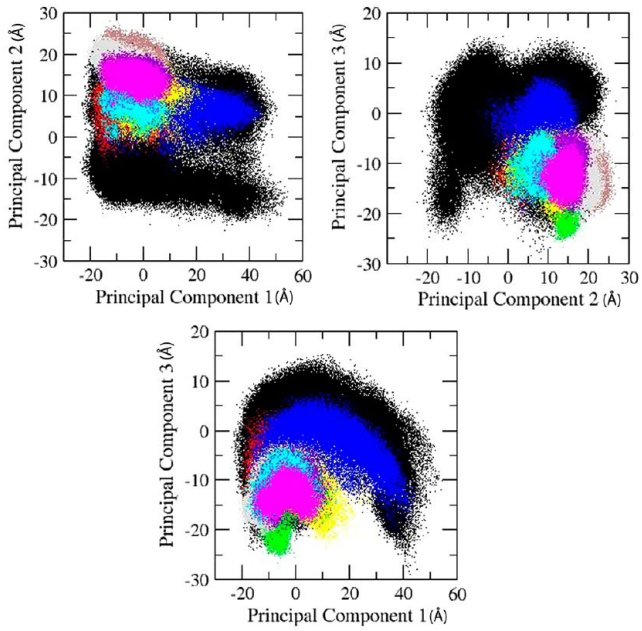

Figure 4. Top three principal components of the motions of the active site residues of the different CypA ensembles: (free) black, (cis) red, (transition state) green, (trans) blue, (A) cyan, (B) magenta, (C) gray, (D) violet, (E) brown, and (F) yellow. The active site residues are Arg 55, Phe 60, Met 61, Gln 63, Gly 74, Gly 75, Glu 81, Lys 82, Ala 101, Asn 102, Ala 103, Thr 107, Gly 109, Ser 110, Gln 111, Phe 113, Leu 122, and His 126.

the presence of compounds (A–F) in the active site dramatically changes the internal motions of CypA. For all of the compounds (A–F), the principal modes overlap considerably with those of the transition state and cis configurations. Our studies suggest that the enzyme conformations of the cis and transition state complexes are the most selective for inhibitor binding and can, therefore, be the most suitable for designing novel drug candidates. This could be a general phenomenon, since it has been known for a long time that transition state mimics tend to always lead to better inhibitors. Our studies provide a molecular level description of this phenomenon. The active site residues adopt conformations that bind the substrate in the different bound states and are the most relevant to the activity of the enzyme. Lack of ergodicity in the sampling of the free enzyme could lead to limitations in sampling conformations that may or may not be relevant to the catalytic function of the enzyme. One could directly use the transition state or cis ensemble of enzyme conformations in structure-based drug design. However, the challenge in using the transition state ensemble of the enzyme in rational drug design is that the transition state of the reaction is not always well-defined a priori. In the case of CypA, which does not involve bond breaking or formation during catalysis, the transition state is easily identifiable and modeled using classical molecular mechanics.

Conformational Dynamics of the Nonpolar and Polar Cavities and Implications for Drug Design. The proline hydrophobic binding cavity samples a broader range of configurations in the free enzyme than in the trans, cis, and transition state complexes (Figure 5A). The hydrophobic cavity of the transition state ensemble is more localized than the cis and trans ensembles. The highly localized hydrophobic pocket of the proline-binding pocket is partly responsible for the tighter binding of the transition state configuration of the substrate by CypA. All of the inhibitors also occupy the localized hydrophobic binding pocket of CypA. The con-

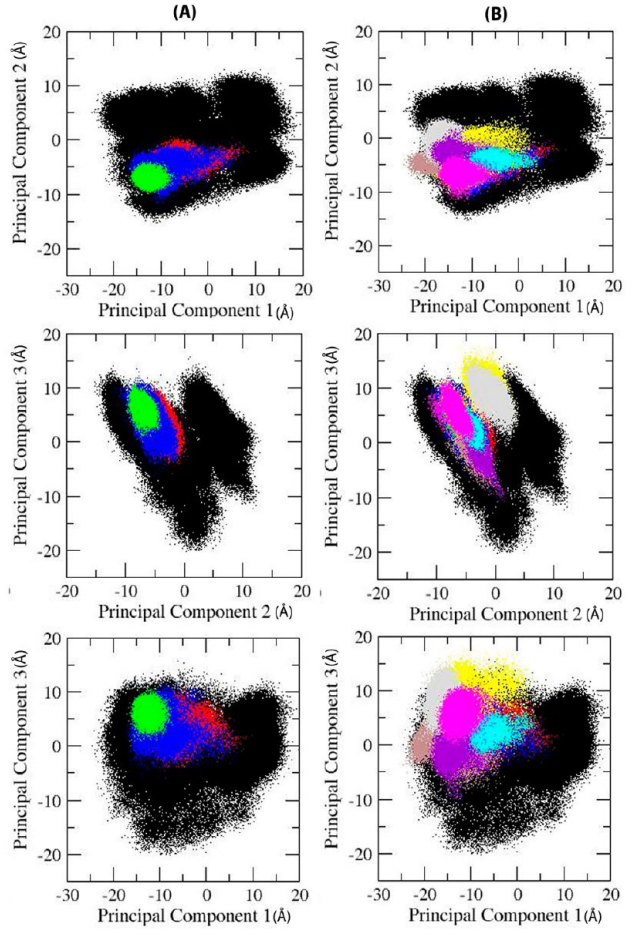

Figure 5. Top three principal components of only the hydrophobic pocket residues of the CypA ensembles of (A) (substrate-free) black, (cis) red, (transition state) green, and (trans) blue and (B) inhibitor-bound CypA: (A) cyan, (B) magenta, (C) gray, (D) violet, (E) brown, and (F) yellow. The hydrophobic pocket was defined using the following residues, Arg 55, Phe 60, Met 61, Gln 63, Ala 101, Asn 102, Gln 111, Phe 113, Leu 122, and His 126.

dx.doi.org/10.1021/ci300432w | J. Chem. Inf. Model. 2013, 53, 403–410

formations of the hydrophobic cavity of the enzyme of the inhibitor-bound complexes cluster around the same area along the top three principal modes (Figure 5B) and are similar to that of the cis, trans, and transition state enzyme ensembles.

Similarly, the hydrophilic cavity of the bound complexes of the different states of the substrate and inhibitors also samples a smaller region of conformational space than that of the substrate-free enzyme (Figure 6). The one exception is the

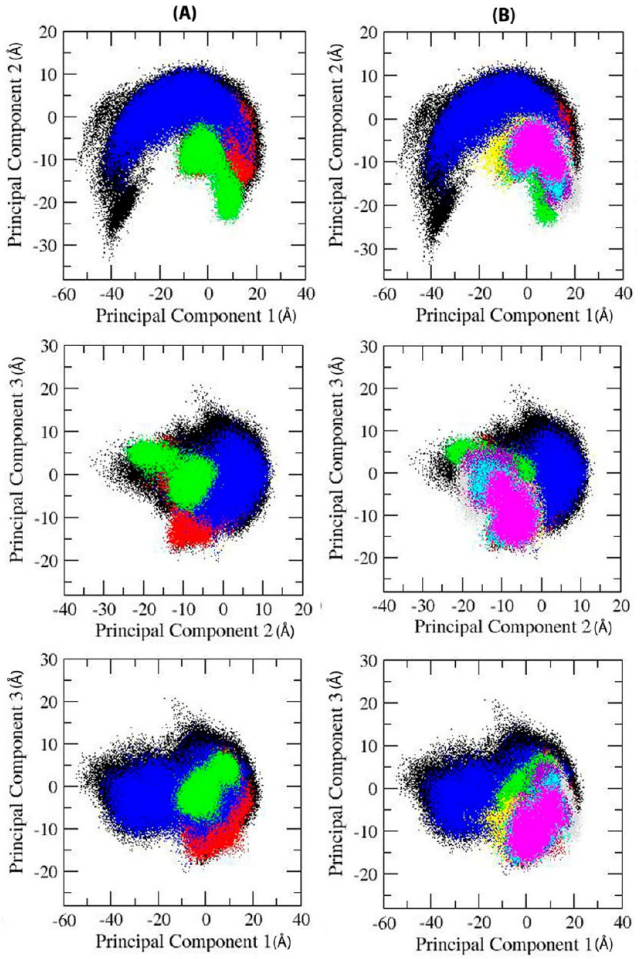

Figure 6. Top three principal components of the hydrophilic pocket residues of the CypA ensembles of (A) (substrate-free) black, (cis) red, (transition state) green, and (trans) blue CypA and (B) inhibitor-bound CypA: (A) cyan, (B) magenta, (C) gray, (D) violet, (E) brown, and (F) yellow. The hydrophilic pocket was defined using the following residues: Gly 74, Gly 75, Glu 81, Lys 82, Ala 101, Asn 102, Ala 103, Thr 107, Gly 109, Ser 110, and Gln 111.

enzyme ensemble of the substrate in the trans configuration, which samples as much space as the free enzyme. It is worth noting that the substrate in the trans configuration has the weakest binding affinity to the enzyme than the cis and transition state configurations. The conformations of the hydrophilic cavity of the inhibitors are similar to those of the transition state and the cis configuration of the substrate (Figure 6B). It is interesting to note that the hydrophilic cavity is not occupied by the peptide substrate analogue in the different states and is occupied by only some of the inhibitors. Instead, there are localized water molecules in the hydrophilic cavity.

Molecular dynamics simulations reveal that the inhibitors occupy mainly the proline binding hydrophobic pocket and the polar channel. In the crystal structure, as well as in the simulation, compound B partially occupies the hydrophilic pocket with the amino-benzyl group, whereas water molecules fill the polar pocket in the other complexes (Figure 7). Figure 7

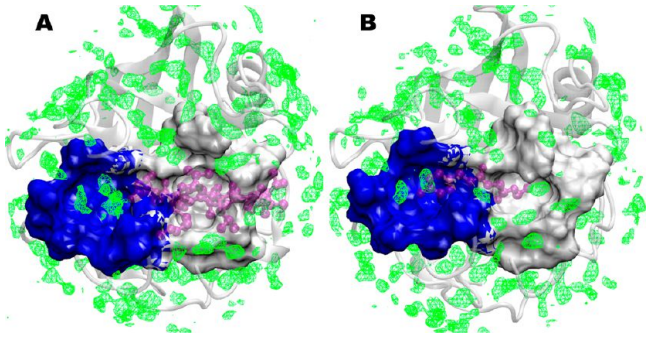

Figure 7. Hydration density around inhibitor-bound complexes of CypA for inhibitors (A) A and (B) B. Active site residues are shown in surface with hydrophilic and hydrophobic cavities colored in blue and white, respectively. The inhibitors are in purple transparent ball and stick model. The green colored mesh represents the hydration density approximately five times that of bulk water.

shows the hydration density maps of CypA in complex with compounds A (CsA) and B. CsA does not occupy the hydrophilic pocket, and this pocket is filled with localized water molecules. Compound B partially occupies the hydrophilic pocket and displaces some of the localized water molecules in the hydrophilic pocket. Mikol et al.[41] reported that a CsA (compound A) derivative that occupies the polar pocket by displacing a structural water molecule had significantly decreased potency as compared to CsA. In this later case, the unfavorable desolvation free energy and conformational destabilization energy of the modified CsA contributed to diminished binding affinity. Several studies have investigated the importance of interfacial water molecules in protein−ligand complexes.[50−53] In some cases, careful redesigning of a ligand to displace localized water could lead to better affinity. For example, HIV protease inhibitors that were designed to displace and mimic the interactions of the bound water molecules were found to bind more strongly to the protein and improved the biological activity. A possible gain in entropy upon the water release and the redesign of the flexible inhibitor into a conformationally restricted one that matches the shape of the active site contributed to the improved affinity.[54] Similarly, the scytalone dehydratase inhibitors, such as salicylamide analogue inhibitors, that displace one of the crystallographic water molecules have higher inhibitory activity.[55] Many examples have been reported in the literature wherein ligands are designed to form direct hydrogen bonds or displace water molecules in order to achieve higher binding affinity.[52,56] Therefore, it appears that the biological activity of drugs could be improved by minimizing the loss of the conformational entropy of the compounds that can form strong direct hydrogen bonding interactions with the receptor.[57] The gain in binding affinity upon displacing localized water molecules can potentially be achieved if the displacing group is preorganized to bind in the cavity with little or no loss in entropy and the interaction energies and gain in entropy of

dx.doi.org/10.1021/ci300432w | J. Chem. Inf. Model. 2013, 53, 403−410

releasing the localized water molecules overcompensate for the loss in conformational entropy.

Our results suggest that a compound with a bulky nonpolar group, similar in size to the nonpolar pocket, and a polar group, similar in size to the polar cavity, that are on opposite sides of a polar linker with the appropriate length are necessary to achieve high selectivity for CypA. Furthermore, minimizing the number of rotatable bonds in order to reduce the loss in conformational entropy upon binding could enhance the affinity. More detailed free energy calculations[15] can be carried out on lead compounds to further optimize binding and selectivity in silico.

CONCLUDING REMARKS

The conformations of an enzyme can vary considerably as its substrate goes from the reactant state through the transition state to the product state. The results of our molecular dynamics simulations and principal component analysis reveal that the binding site of CypA recognizes the peptide substrate analogue in the trans, transition state, and cis configurations mainly via conformational selection. Moreover, the enzyme transition state ensemble of conformations exhibit less conformational fluctuation than any other ensemble and is the least populated by the free enzyme. Inhibitors of CypA were shown to bind more favorably to enzyme conformations that are similar to those of the cis and transition state complexes. Our results reveal the importance of the polar pocket in human CypA and the occupied water molecules in designing potent inhibitors. These results allow us to argue that the enzyme cis and transition state ensembles contain the most relevant conformations for developing and optimizing selective inhibitors in structure-based drug design.

COMPUTATIONAL METHODS

A 1.58 Å resolution crystal structure with PDB ID 1AWR[58] was used to carry out the simulations of the substrate-free and substrate-bound CypA. All simulations are carried out using AMBER 10 suite of programs[59] in explicit TIP3P[60] water model in a periodic octahedron box, using the modified version of the all-atom Cornell et al.[61] force field and the reoptimized dihedral parameters for the peptide ω-bond.[62] The systems were brought to electrostatic neutrality by adding chloride ions. A total of ten MD simulations were carried out: a 340 ns simulation of substrate-free CypA, three simulations of CypA-substrate complexes, each ran for 50 ns, with the peptide ω-bond angle of the -Ala-Pro- motif of a well-studied substrate analogue (Ace-Ala-Ala-Pro-Phe-Nme) in the trans, cis, or transition state configurations, and six simulations of CypA–inhibitor complexes (Figure 1), each ran for 30 ns. The substrate analogue was derived from the original substrate, HAGPIA, in the PDB file by keeping the backbone and common side chain atoms and allowing *xleap* to add the missing atoms. The crystal structure contains the substrate in the trans configuration. The substrate was kept in the transition state configurations by restraining the peptide ω-bond angle using a flat-bottom well potential at ~90° with a force constant of 1000 kcal/(mol rad^2). The simulations of the CypA–substrate complexes when the substrate was in cis and trans configurations were carried out with no restraints, since the two ground state configurations are separated by a high barrier. First, the systems are minimized to achieve the lowest-energy conformations. The systems were equilibrated using MD for 200 ps with a 50 kcal/(mol Å^2) harmonic constraint applied to all of CypA, bringing the temperature up to 300 K. A second equilibration was carried out at 300 K for 200 ps with a 25 kcal/(mol Å^2) harmonic constraint applied to all of the atoms of CypA. The final equilibration was carried out for 200 ps without any harmonic constraints. During the simulations, an integration time step of 0.002 ps was used to solve the Newton's equation of motion. The Particle Mesh Ewald method[63] was used to evaluate long-range electrostatic interactions, and a cutoff of 9.0 Å was used for nonbonded interactions. The SHAKE algorithm[64] was used to restrain all bonds involving hydrogen atoms. The simulations were carried out at a constant temperature of 300 K and a constant pressure of 1 bar. The temperature was regulated using the Langevin thermostat with a collision frequency of 1.0 ps^{-1}. The trajectories were saved every 500 steps (1 ps).

AutoDock Vina[49] was used to dock compounds C–F into the active site of CypA and Gauss View 3.09[65] was used to build the different inhibitors shown in Figure 1. The inhibitors represent a collection of nonpeptidomimetic CypA inhibitors from the literature, with each inhibitor representing the compound with the highest activity within its class. The nonpolar hydrogen atoms were merged to the corresponding heavy atoms. Gasteiger charges were added to the protein and inhibitors using AutoDock ADT. The inhibitors were docked to an ensemble of CypA conformations, obtained from the molecular dynamics simulation. Every other 10 conformations of CypA from the MD trajectories were used in the docking studies. The docking parameters were set as follows: the grid spacing was 1.0 Å; the box size was 25 Å in each dimension, and the center of the box was chosen so as to have all of the active site residues within the box. The maximum number of binding modes saved was set to 10. The configuration of the inhibitor in the active site with the lowest binding energy was assumed to be the best binding mode for that conformation of CypA. The most probable binding mode was assumed to be the correct binding mode and was used to carry out molecular dynamics simulation on the CypA–inhibitor complex. The MD simulations were carried out as described above. The force field parameters for the inhibitors were derived using the Antechamber module in Amber. The ability of AutoDock Vina to provide the correct binding modes of compounds C–F was validated by redocking compounds A and B to the single conformation of the respective crystal structures and an ensemble of conformations of CypA that was generated using molecular dynamics. The binding modes obtained using AutoDock Vina were similar to the binding modes of compounds A and B in the active site of CypA in the crystal structures (Supporting Information Figure S1).

ASSOCIATED CONTENT

Supporting Information

Validation of AutoDock Vina by redocking compound B into the active site of CypA. This material is available free of charge via the Internet at http://pubs.acs.org.

AUTHOR INFORMATION

Corresponding Author

*Mailing address: Department of Chemistry, Georgia State University, P.O. Box 4098, Atlanta, GA 30302-4098. E-mail: dhamelberg@gsu.edu. Tel.: 404-413-5564. Fax: 404-413-5505.

Notes

The authors declare no competing financial interest.

■ ACKNOWLEDGMENTS

This work is supported in part by the National Science Foundation (MCB-0953061) and Georgia Cancer Coalition. L.C.M is a Molecular Basis of Disease Fellow and is supported by the Molecular Basis of Disease Program at Georgia State University. This work was also supported by Georgia State's IBM System p7 supercomputer, acquired through a partnership of the Southeastern Universities Research Association and IBM supporting the SURAgrid initiative.

■ REFERENCES

(1) Handschumacher, R. E.; Harding, M. W.; Rice, J.; Drugge, R. J.; Speicher, D. W. Cyclophilin: a specific cytosolic binding protein for cyclosporin A. *Science* **1984**, *226*, 544−547.

(2) Dornan, J.; Taylor, P.; Walkinshaw, M. D. Structures of immunophilins and their ligand complexes. *Curr. Top. Med. Chem.* **2003**, *3*, 1392−1409.

(3) Galat, A. Peptidylprolyl cis/trans isomerases (immunophilins): biological diversity–targets–functions. *Curr. Top. Med. Chem.* **2003**, *3*, 1315−1347.

(4) Fischer, G.; Wittmann-Liebold, B.; Lang, K.; Kiefhaber, T.; Schmid, F. X. Cyclophilin and peptidyl-prolyl cis-trans isomerase are probably identical proteins. *Nature* **1989**, *337*, 476−478.

(5) Luban, J.; Bossolt, K. L.; Franke, E. K.; Kalpana, G. V.; Goff, S. P. Human immunodeficiency virus type 1 Gag protein binds to cyclophilins A and B. *Cell* **1993**, *73*, 1067−1078.

(6) Gamble, T. R.; Vajdos, F. F.; Yoo, S.; Worthylake, D. K.; Houseweart, M.; Sundquist, W. I.; Hill, C. P. Crystal structure of human cyclophilin A bound to the amino-terminal domain of HIV-1 capsid. *Cell* **1996**, *87*, 1285−1294.

(7) Shen, J.; Person, M. D.; Zhu, J.; Abbruzzese, J. L.; Li, D. Protein expression profiles in pancreatic adenocarcinoma compared with normal pancreatic tissue and tissue affected by pancreatitis as detected by two-dimensional gel electrophoresis and mass spectrometry. *Cancer Res.* **2004**, *64*, 9018−9026.

(8) Howard, B. A.; Zheng, Z.; Campa, M. J.; Wang, M. Z.; Sharma, A.; Haura, E.; Herndon, J. E., 2nd; Fitzgerald, M. C.; Bepler, G.; Patz, E. F., Jr. Translating biomarkers into clinical practice: prognostic implications of cyclophilin A and macrophage migratory inhibitory factor identified from protein expression profiles in non-small cell lung cancer. *Lung Cancer* **2004**, *46*, 313−323.

(9) Li, Z.; Zhao, X.; Bai, S.; Wang, Z.; Chen, L.; Wei, Y.; Huang, C. Proteomics identification of cyclophilin a as a potential prognostic factor and therapeutic target in endometrial carcinoma. *Mol. Cell Proteomics* **2008**, *7*, 1810−1823.

(10) Theuerkorn, M.; Fischer, G.; Schiene-Fischer, C. Prolyl cis/trans isomerase signalling pathways in cancer. *Curr. Opin. Pharmacol.* **2011**, *11*, 281−287.

(11) Luo, C.; Luo, H.; Zheng, S.; Gui, C.; Yue, L.; Yu, C.; Sun, T.; He, P.; Chen, J.; Shen, J.; Luo, X.; Li, Y.; Liu, H.; Bai, D.; Yang, Y.; Li, F.; Zuo, J.; Hilgenfeld, R.; Pei, G.; Chen, K.; Shen, X.; Jiang, H. Nucleocapsid protein of SARS coronavirus tightly binds to human cyclophilin A. *Biochem. Biophys. Res. Commun.* **2004**, *321*, 557−565.

(12) Capano, M.; Virji, S.; Crompton, M. Cyclophilin-A is involved in excitotoxin-induced caspase activation in rat neuronal B50 cells. *Biochem. J.* **2002**, *363*, 29−36.

(13) Dawson, T. M.; Steiner, J. P.; Lyons, W. E.; Fotuhi, M.; Blue, M.; Snyder, S. H. The immunophilins, FK506 binding protein and cyclophilin, are discretely localized in the brain: relationship to calcineurin. *Neuroscience* **1994**, *62*, 569−580.

(14) Daum, S.; Schumann, M.; Mathea, S.; Aumuller, T.; Balsley, M. A.; Constant, S. L.; de Lacroix, B. F.; Kruska, F.; Braun, M.; Schiene-Fischer, C. Isoform-specific inhibition of cyclophilins. *Biochemistry* **2009**, *48*, 6268−6277.

(15) Sambasivarao, S. V.; Acevedo, O. Computational Insight into Small Molecule Inhibition of Cyclophilins. *J. Chem. Inf. Model.* **2011**, *51*, 475−482.

(16) Acevedo, O.; Ambrose, Z.; Flaherty, P. T.; Aamer, H.; Jain, P.; Sambasivarao, S. V. Identification of HIV inhibitors guided by free energy perturbation calculations. *Curr. Pharm. Des.* **2012**, *18*, 1199−1216.

(17) Siekierka, J. J.; Hung, S. H.; Poe, M.; Lin, C. S.; Sigal, N. H. A cytosolic binding protein for the immunosuppressant FK506 has peptidyl-prolyl isomerase activity but is distinct from cyclophilin. *Nature* **1989**, *341*, 755−757.

(18) Sedrani, R.; Kallen, J.; Martin Cabrejas, L. M.; Papageorgiou, C. D.; Senia, F.; Rohrbach, S.; Wagner, D.; Thai, B.; Jutzi Eme, A. M.; France, J.; Oberer, L.; Rihs, G.; Zenke, G.; Wagner, J. Sanglifehrin-cyclophilin interaction: degradation work, synthetic macrocyclic analogues, X-ray crystal structure, and binding data. *J. Am. Chem. Soc.* **2003**, *125*, 3849−3859.

(19) Calne, R. Y.; Collier, D. S.; Lim, S.; Pollard, S. G.; Samaan, A.; White, D. J.; Thiru, S. Rapamycin for immunosuppression in organ allografting. *Lancet* **1989**, *334* (8656), 227−227.

(20) Hojo, M.; Morimoto, T.; Maluccio, M.; Asano, T.; Morimoto, K.; Lagman, M.; Shimbo, T.; Suthanthiran, M. Cyclosporine induces cancer progression by a cell-autonomous mechanism. *Nature* **1999**, *397*, 530−534.

(21) Jorgensen, W. L. The many roles of computation in drug discovery. *Science* **2004**, *303*, 1813−1818.

(22) Leach, A. R.; Shoichet, B. K.; Peishoff, C. E. Prediction of protein-ligand interactions. Docking and scoring: successes and gaps. *J. Med. Chem.* **2006**, *49*, 5851−5855.

(23) Perola, E.; Walters, W. P.; Charifson, P. S. A detailed comparison of current docking and scoring methods on systems of pharmaceutical relevance. *Proteins* **2004**, *56*, 235−249.

(24) Halgren, T. A.; Murphy, R. B.; Friesner, R. A.; Beard, H. S.; Frye, L. L.; Pollard, W. T.; Banks, J. L. Glide: a new approach for rapid, accurate docking and scoring. 2. Enrichment factors in database screening. *J. Med. Chem.* **2004**, *47*, 1750−1759.

(25) Zhou, Z.; Felts, A. K.; Friesner, R. A.; Levy, R. M. Comparative performance of several flexible docking programs and scoring functions: enrichment studies for a diverse set of pharmaceutically relevant targets. *J. Chem. Inf. Model.* **2007**, *47*, 1599−1608.

(26) Cavasotto, C. N.; Kovacs, J. A.; Abagyan, R. A. Representing receptor flexibility in ligand docking through relevant normal modes. *J. Am. Chem. Soc.* **2005**, *127*, 9632−9640.

(27) Zavodszky, M. I.; Lei, M.; Thorpe, M. F.; Day, A. R.; Kuhn, L. A. Modeling correlated main-chain motions in proteins for flexible molecular recognition. *Proteins* **2004**, *57*, 243−261.

(28) Schnecke, V.; Swanson, C. A.; Getzoff, E. D.; Tainer, J. A.; Kuhn, L. A. Screening a peptidyl database for potential ligands to proteins with side-chain flexibility. *Proteins* **1998**, *33*, 74−87.

(29) Alberts, I. L.; Todorov, N. P.; Dean, P. M. Receptor flexibility in de novo ligand design and docking. *J. Med. Chem.* **2005**, *48*, 6585−6596.

(30) Adcock, S. A.; McCammon, J. A. Molecular dynamics: survey of methods for simulating the activity of proteins. *Chem. Rev.* **2006**, *106*, 1589−1615.

(31) Lin, J. H.; Perryman, A. L.; Schames, J. R.; McCammon, J. A. Computational drug design accommodating receptor flexibility: the relaxed complex scheme. *J. Am. Chem. Soc.* **2002**, *124*, 5632−5633.

(32) Perryman, A. L.; Lin, J. H.; Andrew McCammon, J. Optimization and computational evaluation of a series of potential active site inhibitors of the V82F/I84V drug-resistant mutant of HIV-1 protease: an application of the relaxed complex method of structure-based drug design. *Chem. Biol. Drug. Des.* **2006**, *67*, 336−345.

(33) Lin, J. H.; Perryman, A. L.; Schames, J. R.; McCammon, J. A. The relaxed complex method: Accommodating receptor flexibility for drug design with an improved scoring scheme. *Biopolymers* **2003**, *68*, 47−62.

(34) Craig, I. R.; Essex, J. W.; Spiegel, K. Ensemble docking into multiple crystallographically derived protein structures: an evaluation based on the statistical analysis of enrichments. *J. Chem. Inf. Model.* **2010**, *50*, 511−524.

(35) Rao, S.; Sanschagrin, P. C.; Greenwood, J. R.; Repasky, M. P.; Sherman, W.; Farid, R. Improving database enrichment through ensemble docking. *J. Comput. Aided. Mol. Des.* **2008**, *22*, 621−627.
(36) Limongelli, V.; Marinelli, L.; Cosconati, S.; Braun, H. A.; Schmidt, B.; Novellino, E. Ensemble-docking approach on BACE-1: pharmacophore perception and guidelines for drug design. *Chem. Med. Chem.* **2007**, *2*, 667−678.
(37) Huang, S. Y.; Zou, X. Ensemble docking of multiple protein structures: considering protein structural variations in molecular docking. *Proteins* **2007**, *66*, 399−421.
(38) Nichols, S. E.; Baron, R.; Ivetac, A.; McCammon, J. A. Predictive power of molecular dynamics receptor structures in virtual screening. *J. Chem. Inf. Model.* **2011**, *51*, 1439−1446.
(39) McGovern, S. L.; Shoichet, B. K. Information decay in molecular docking screens against holo, apo, and modeled conformations of enzymes. *J. Med. Chem.* **2003**, *46*, 2895−2907.
(40) Wolfenden, R. Transition State Analog Inhibitors and Enzyme Catalysis. *Annu. Rev. Biophys. Bioeng.* **1976**, *5*, 271−306.
(41) Mikol, V.; Papageorgiou, C.; Borer, X. The role of water molecules in the structure-based design of (5-hydroxynorvaline)-2-cyclosporin: synthesis, biological activity, and crystallographic analysis with cyclophilin A. *J. Med. Chem.* **1995**, *38*, 3361−3367.
(42) Ni, S.; Yuan, Y.; Huang, J.; Mao, X.; Lv, M.; Zhu, J.; Shen, X.; Pei, J.; Lai, L.; Jiang, H.; Li, J. Discovering potent small molecule inhibitors of cyclophilin A using de novo drug design approach. *J. Med. Chem.* **2009**, *52*, 5295−5298.
(43) Wu, Y. Q.; Belyakov, S.; Choi, C.; Limburg, D.; Thomas, I. B.; Vaal, M.; Wei, L.; Wilkinson, D. E.; Holmes, A.; Fuller, M.; McCormick, J.; Connolly, M.; Moeller, T.; Steiner, J.; Hamilton, G. S. Synthesis and biological evaluation of non-peptidic cyclophilin ligands. *J. Med. Chem.* **2003**, *46*, 1112−1115.
(44) Guichou, J.-F.; Colliandre, L.; Ahmed-Belkacem, H.; Pawlotsky, J.-M. *New inhibitors of cyclophilins and uses thereof*. Patent WO2011076784, 2011.
(45) Ma, B.; Nussinov, R. Enzyme dynamics point to stepwise conformational selection in catalysis. *Curr. Opin. Chem. Biol.* **2010**, *14*, 652−659.
(46) Kollman, P. A.; Massova, I.; Reyes, C.; Kuhn, B.; Huo, S.; Chong, L.; Lee, M.; Lee, T.; Duan, Y.; Wang, W.; Donini, O.; Cieplak, P.; Srinivasan, J.; Case, D. A.; Cheatham, T. E., 3rd Calculating structures and free energies of complex molecules: combining molecular mechanics and continuum models. *Acc. Chem. Res.* **2000**, *33*, 889−897.
(47) Doshi, U.; McGowan, L. C.; Ladani, S. T.; Hamelberg, D. Resolving the complex role of enzyme conformational dynamics in catalytic function. *Proc. Natl. Acad. Sci. U S A* **2012**, *109*, 5699−5704.
(48) Hamelberg, D.; McCammon, J. A. Mechanistic insight into the role of transition-state stabilization in cyclophilin A. *J. Am. Chem. Soc.* **2009**, *131*, 147−152.
(49) Trott, O.; Olson, A. J. AutoDock Vina: Improving the speed and accuracy of docking with a new scoring function, efficient optimization, and multithreading. *J. Comput. Chem.* **2010**, *30*, 455−461.
(50) Lu, Y.; Yang, C. Y.; Wang, S. Binding free energy contributions of interfacial waters in HIV-1 protease/inhibitor complexes. *J. Am. Chem. Soc.* **2006**, *128*, 11830−11839.
(51) Garcia-Sosa, A. T.; Mancera, R. L. Free Energy Calculations of Mutations Involving a Tightly Bound Water Molecule and Ligand Substitutions in a Ligand-Protein Complex. *Mol. Inf.* **2010**, *29*, 589−600.
(52) de Beer, S. B.; Vermeulen, N. P.; Oostenbrink, C. The role of water molecules in computational drug design. *Curr. Top. Med. Chem.* **2010**, *10*, 55−66.
(53) Hamelberg, D.; McCammon, J. A. Standard free energy of releasing a localized water molecule from the binding pockets of proteins: double-decoupling method. *J. Am. Chem. Soc.* **2004**, *126*, 7683−7689.
(54) Lam, P. Y.; Jadhav, P. K.; Eyermann, C. J.; Hodge, C. N.; Ru, Y.; Bacheler, L. T.; Meek, J. L.; Otto, M. J.; Rayner, M. M.; Wong, Y. N.; et al. Rational design of potent, bioavailable, nonpeptide cyclic ureas as HIV protease inhibitors. *Science* **1994**, *263*, 380−384.
(55) Chen, J. M.; Xu, S. L.; Wawrzak, Z.; Basarab, G. S.; Jordan, D. B. Structure-based design of potent inhibitors of scytalone dehydratase: displacement of a water molecule from the active site. *Biochemistry* **1998**, *37*, 17735−17744.
(56) Li, Z.; Lazaridis, T. Water at biomolecular binding interfaces. *Phys. Chem. Chem. Phys.* **2007**, *9*, 573−581.
(57) Connelly, P. R.; Aldape, R. A.; Bruzzese, F. J.; Chambers, S. P.; Fitzgibbon, M. J.; Fleming, M. A.; Itoh, S.; Livingston, D. J.; Navia, M. A.; Thomson, J. A.; et al. Enthalpy of hydrogen bond formation in a protein-ligand binding reaction. *Proc. Natl. Acad. Sci. USA* **1994**, *91*, 1964−1968.
(58) Vajdos, F. F.; Yoo, S.; Houseweart, M.; Sundquist, W. I.; Hill, C. P. Crystal structure of cyclophilin A complexed with a binding site peptide from the HIV-1 capsid protein. *Protein Sci.* **1997**, *6*, 2297−2307.
(59) Case, D. A.; Darden, T. A.; Cheatham, I., T. E. ; Simmerling, C. L.; Wang, J.; Duke, R. E.; Luo, R.; Crowley, M.; Walker, R. C.; Zhang, W.; Merz, K. M.; Wang, B.; Hayik, S.; Roitberg, A.; Seabra, G.; Kolossváry, I.; Wong, K. F.; Paesani, F.; Vanicek, J.; Wu, X.; Brozell, S. R.; Steinbrecher, T.; Gohlke, H.; Yang, L.; Tan, C.; Mongan, J.; Hornak, V.; Cui, G.; Mathews, D. H.; Seetin, M.G.; ; Sagui, C.; Babin, V.; Kollman, P. A. *AMBER 10*; University of California, San Francisco; 2008.
(60) Jorgensen, W. L.; Chandrasekhar, J.; Madura, J. D.; Impey, R. W.; Klein, M. L. Comparison of simple potential functions for simulating liquid water. *J. Chem. Phys.* **1983**, *79*, 926−935.
(61) Cornell, W. D.; Cieplak, P.; Christopher, I. B.; Gould, I. R.; Merz, J. K. M.; Ferguson, D. M.; Spellmeyer, D. C.; Fox, T.; Caldwell, J. W.; Kollman, P. A. A Second Generation Force Field for the Simulation of Proteins, Nucleic Acids, and Organic Molecules. *J. Am. Chem. Soc.* **1995**, *117*, 5179−5197.
(62) Urmi, D.; Hamelberg, D. Reoptimization of the AMBER Force Field Parameters for Peptide Bond (Omega) Torsions Using Accelerated Molecular Dynamics. *J. Phys. Chem. B* **2009**, *113*, 16590−16595.
(63) Darden, T.; York, D.; Pedersen, L. Particle mesh Ewald: An N·log(N) method for Ewald sums in large systems. *J. Chem. Phys.* **1993**, *98*, 10089−10092.
(64) Ryckaert, J. P.; Ciccotti, G.; Berendsen, H. J. C. Numerical integration of the cartesian equations of motion of a system with constraints: molecular dynamics of n-alkanes. *J. Comput. Phys.* **1977**, *23*, 327−341.
(65) Dennington, R., II; Keith, T.; Millam, J. *Gaussview*, version 3.09; Semichem, Inc., Shawnee Mission, KS, 2003.